Supporting Information

Swanson et al. 10.1073/pnas.1106536108

SI Materials and Methods

Structure Determination. X-ray diffraction data were collected at the 17-ID beamline (Industrial Macromolecular Crystallography Association - Collaborative Access Team, Advanced Photon Source, Argonne National Laboratory, Argonne, IL) on a Pilatus detector. The data were integrated with XDS (1) and scaled with SCALA (2, 3). Due to severe anisotropy of the diffraction in the c* direction of the crystals, data were corrected using ellipsoidal truncation cutoffs and isotropic B-factor sharpening along each principle axis as implemented in the Diffraction Anisotropy Server (http://services.mbi.ucla.edu/anisoscale/). Initial phasing was performed by molecular replacement with PHASER (3, 4) using as a search model a modified postfusion PIV3 F protein [Protein Data Bank (PDB) code 1ZTM] in which the six-helix bundle had been replaced with the corresponding region from RSV F (PDB code 3KPE). A search for a single F trimer in the asymmetric unit gave a top solution with a low *Z* score. However, the crystal packing was reasonable and the resulting 2*m*Fo-*d*Fc electron density map showed features of the RSV F protein that were not present in the search model.

The high solvent content (~77%) of the crystals and the presence of a proper intramolecular threefold axis relating the F monomers, allowed improvement of the phases in an unbiased manner with density modification (DM) (3, 5) using a combination of solvent flattening, histogram matching, threefold noncrystallographic symmetry (NCS) averaging, and phase extension without recombination from 7.0 to 3.2 Å. The phases were further improved in a second round of phase extension from 7.0 Å but using the improved threefold matrices, averaging masks, and solvent masks generated at the end of the previous round of DM. The resulting electron density map had strong features for side chains and some obvious backbone carbonyls making model building straightforward (Fig. S3). The trimer was generated from a nearly completely traced monomer using refined matrixes obtained from DM, and Refmac (3, 6) was used for structure refinement using tight NCS restrains. After a few cycles of model building and addition of sugars, TLS/restrained refinement was performed. Tight NCS restraints were kept for most of the model throughout refinement with the exception of small regions establishing crystal contacts. In the final rounds, the NCS restraint was loosened for side chains. The final model has R_{work} and R_{free} of 23.1 and 26.6%, respectively (Table S1). The coordinates of the RSV F structure and structure factors have been deposited in the Research Collaboratory for Structural Bioinformatics Protein Database with the identifier code 3rki.

Neutralization Assay.

The RSV microneutralization assay was performed in 96-well microplates using Hep-2 cells and the RSV Long strain. Cells were seeded at a density of 6.5×10^6 cells/mL with 100 μL/well in DMEM supplemented with 5% FBS. The plate was incubated at 37 °C, 5% CO_2 for 3–6 h to allow attachment. Sera were heat inactivated at 56 °C for 30 min, serially diluted in PBS with 5% FBS, and mixed with an equal volume of virus diluted in PBS and 5% FBS. The dilution amount of virus in each assay was selected to yield 80–120 syncytia/well in the absence of neutralizing serum. The virus/serum mix was then incubated for 2 h at 37 °C, 5% CO_2. Medium was then removed from seeded cells and 25 μL/well of the virus/serum mix added to the cells and incubated for 2 h at 37 °C, 5% CO_2. The virus/serum mix was subsequently removed from seeded cells, and 100 μL/well of 0.75% methylcellulose in DMEM supplemented with 5% FBS was transferred onto the cells. The plates were incubated at 37 °C, 5% CO_2 for 40–48 h. The methylcellulose was removed, and the cell monolayer was fixed with 10% buffered formalin for 1 h at room temperature and permeabilized with 0.5% saponin in PBS for 1 h at room temperature. The infected cells were incubated with monoclonal antibodies to F and NP proteins. Bound antibody was detected by incubating with peroxidase-labeled goat anti-mouse IgG and True Blue enzyme substrate. Neutralization titer is the inverse dilution of sample that yields reduction of the syncytia count equivalent to 60% of the count in the absence of a test serum.

1. Kabsch W (2010) XDS. *Acta Crystallogr D Biol Crystallogr* 66:125–132.
2. Evans P (2006) Scaling and assessment of data quality. *Acta Crystallogr D Biol Crystallogr* 62:72–82.
3. Collaborative Computational Project, Number 4 (1994) The CCP4 suite: Programs for protein crystallography. *Acta Crystallogr D Biol Crystallogr* 50:760–763.
4. McCoy AJ, et al. (2007) Phaser crystallographic software. *J Appl Cryst* 40:658–674.
5. Cowtan K (1994) dm: An automated procedure for phase improvement by density modification. *Protein Crystallogr* 31:34–38.
6. Murshudov GN, Vagin AA, Dodson EJ (1997) Refinement of macromolecular structures by the maximum-likelihood method. *Acta Crystallogr D Biol Crystallogr* 53:240–255.

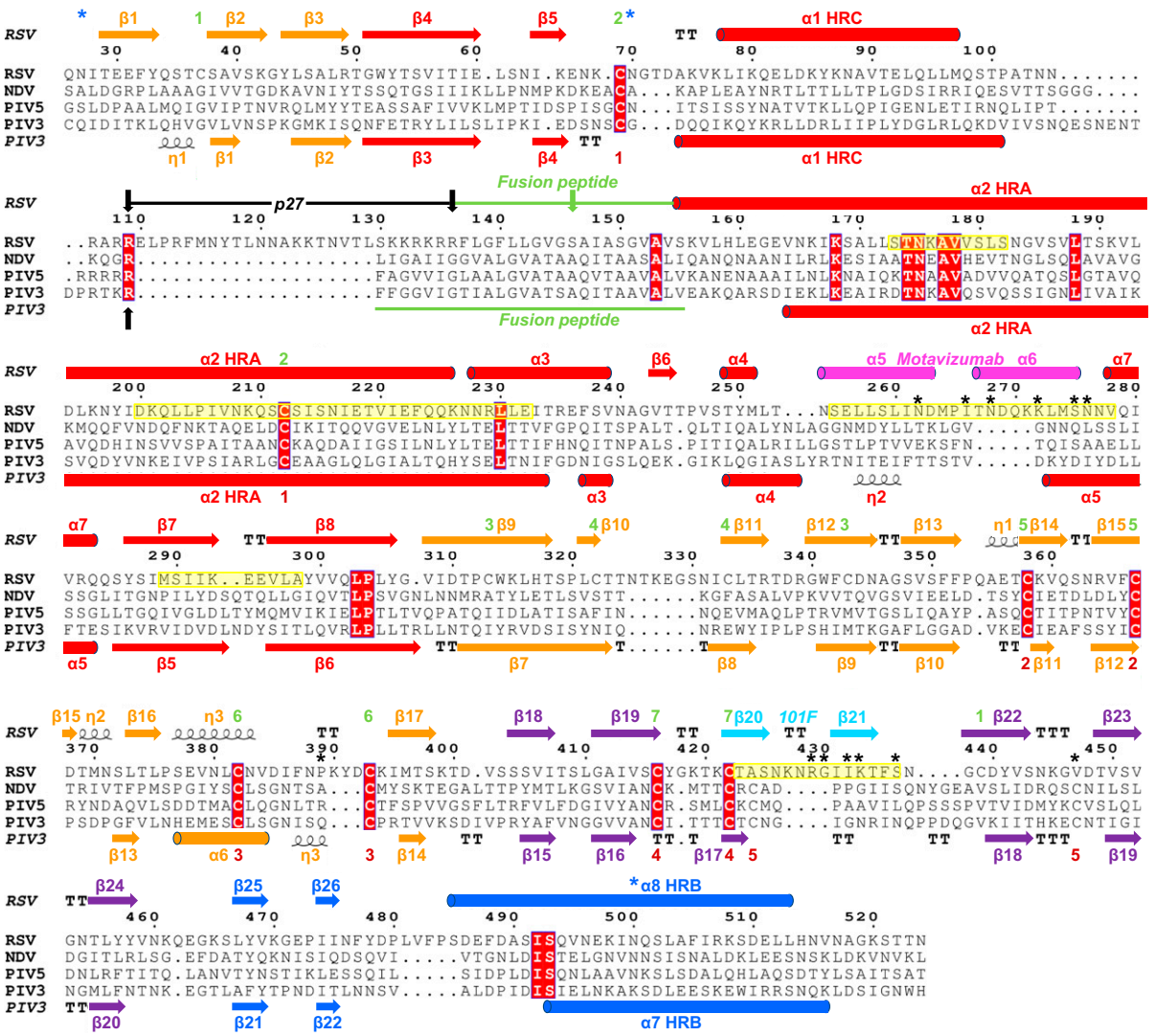

Fig. S1. Structure-based sequence alignment of four F proteins, secondary structure assignment, and key features. The alignment of RSV, NDV, PIV3, and PIV5 F sequences was generated with ClustalW2, adjusted manually on the basis of structural superposition using Lsqkab from the CCP4 suite of programs (1) and displayed using ESPript version 2.2. Features of RSV F are indicated above the sequences; features of PIV3 F are indicated below the sequences. Blue asterisks indicate RSV F glycosylation sites. Secondary structure elements are indicated, with arrows parallel to the sequences designating β sheets, cylinders designating α helices, "TT" designating turns, and coils designating 3_{10} helices. Secondary structure symbols are colored by domain as in Fig. 1, except for RSV helices α5 and α6, which are magenta to indicate that they form the Motavizumab binding site, and β20 and β21, which are cyan to indicate that they form the 101F binding site. Green (RSV) or red (PIV3) numbers designate residues that form disulfide bonds, with the same number for each partner in a disulfide-linked pair. The furin cleavage sites for RSV F and PIV3 F are indicated by black vertical arrows. The RSV F p27 region released from the protein after furin cleavage is indicated by a black bar. The fusion peptides of RSV F and PIV3 F are indicated by green bars. The green arrow indicates the first residue of the F1 fragment in the fusion peptide deletion construct used in this study. Residues that are identical in all four proteins are indicated by red boxes. Peptides used to investigate neutralizing binding sites are highlighted in yellow and neutralization resistance mutations (Table S2) are indicated by black asterisks.

1. Collaborative Computational Project, Number 4 (1994) The CCP4 suite: Programs for protein crystallography. *Acta Crystallogr D Biol Crystallogr* 50:760–763.

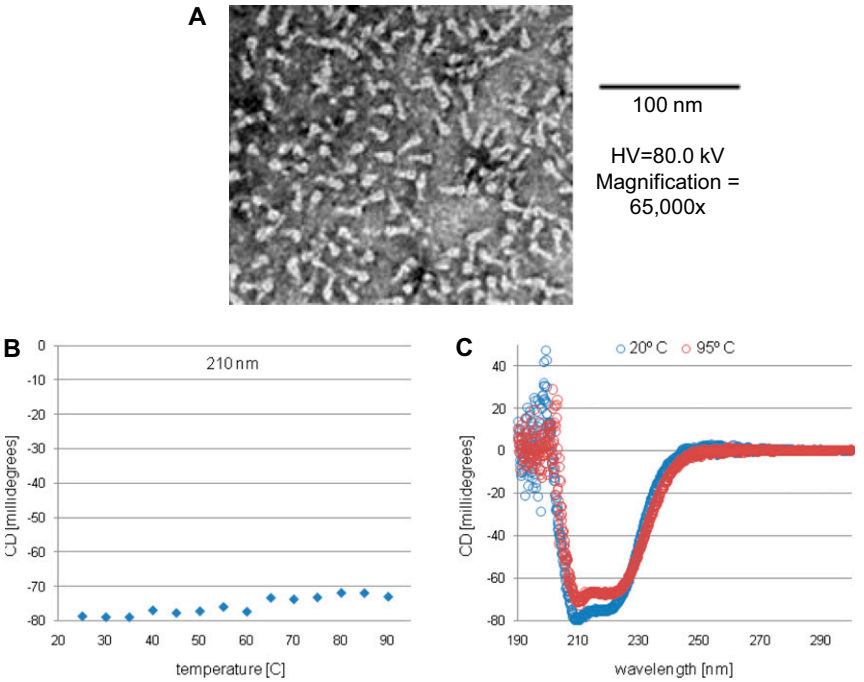

Fig. S2. Electron microscopy and circular dichroism spectroscopy analysis of the RSV F postfusion trimer. (*A*) Electron micrograph of the RSV F protein shows a field of uniform crutch-shaped molecules consistent with the structure of postfusion F proteins. (*B*) CD melting curve of the postfusion RSV F trimer observed at 210 nm, the observed spectral minimum of the folded RSV F protein. The CD rotation, *y* axis, is plotted against temperature, *x* axis. (*C*) CD spectra of the postfusion RSV F trimer at 20 °C and 95 °C (blue and red, respectively). The spectra were recorded from 320 to 190 nm and show at both temperatures characteristic helical minima for a folded protein.

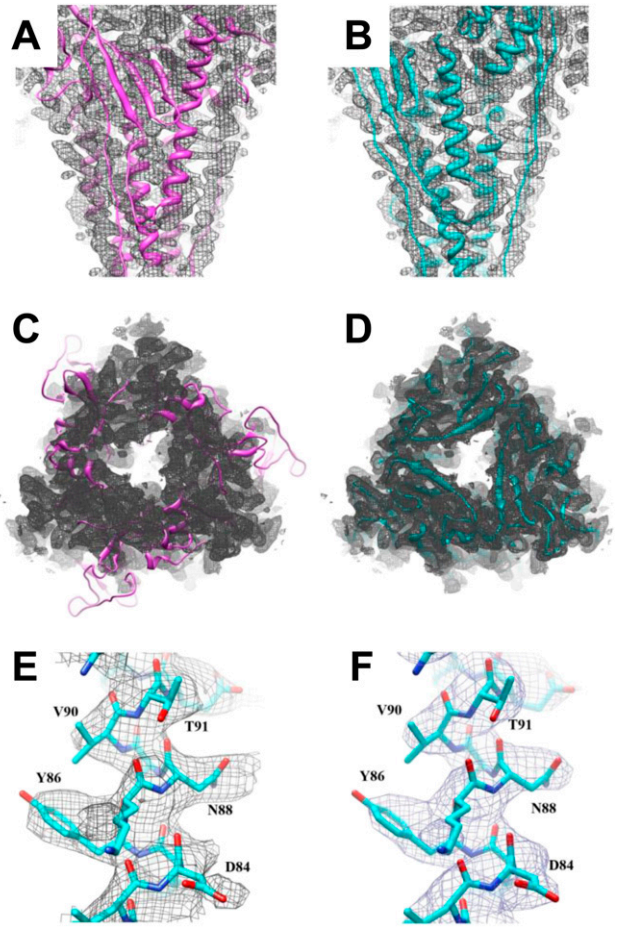

Fig. S3. Representative electron densities. (*A*) Side view. The original molecular replacement solution model (magenta), which contains the PIV3 postfusion head in-frame with the six-helix bundle of RSV F is shown in the initial electron density map (1σ), calculated after iterative real-space NCS threefold averaging, histogram matching, and solvent flattening with phase extension from 7.0 to 3.2 Å and no phase recombination (gray). The head region fits poorly in the electron density. (*C*) Top view. Model and electron density colored as in *A*. (*B*) Side view. The final model of RSV F (blue) shown in the averaged electron density map as described in *A*. (*D*) Top view. Model and electron density colored as in *B*. (*E*) Close up of a representative averaged electron density (gray, 1σ) with the final model in stick representation (blue). (*F*) Same view as in *E* but with final 2*m*Fo-*d*Fc electron density map contoured at 1.5σ (dark blue) (*Materials and Methods*).

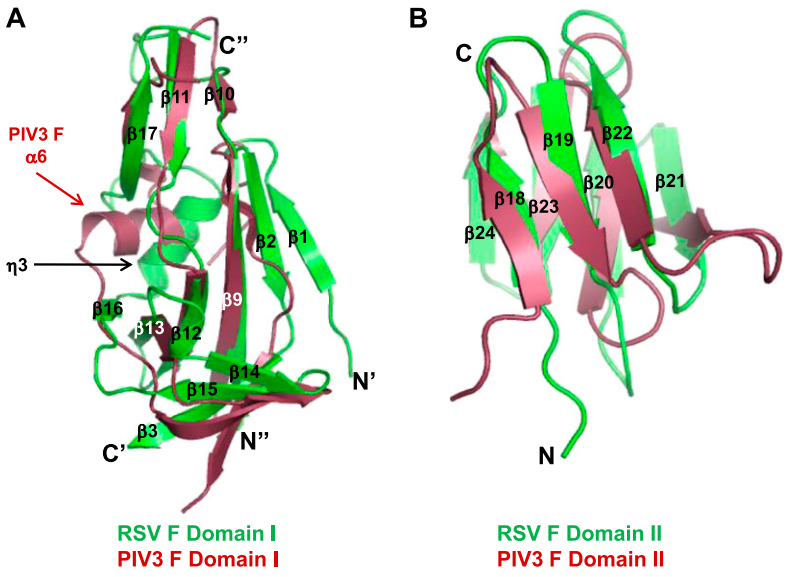

Fig. S4. Superposition of domains I and II of RSV F and PIV3 F. (*A*) Ribbon diagram of domain I from RSV and PIV3 superimposed by matching the common β sheets. The secondary structure elements of RSV F and α6 of PIV3 are labeled. (*B*) Ribbon diagram of domain II from RSV F and PIV3 F superimposed on the basis of common β strands.

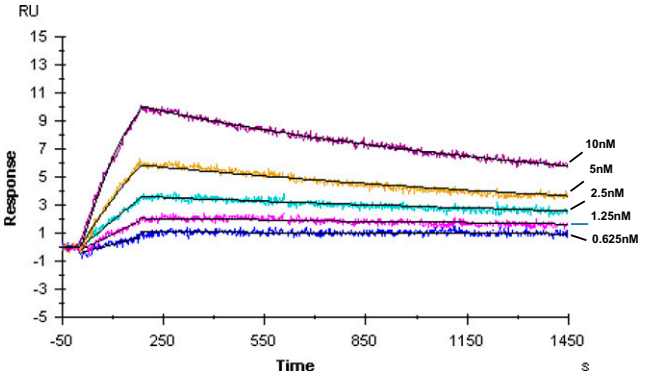

Ka (1/Ms)	Kd (1/s)	KD (M)	Chi² (RU²)	U-value
1.825E+6	7.604E-4	4.166E-10	0.0299	1

Fig. S5. Binding studies by surface plasmon resonance of postfusion RSV F and monoclonal antibody Palivizumab. Palivizumab was immobilized on a sensor chip, and varying concentrations of RSV F were injected with mass absorption response units (RU) monitored as a function of time (sensorgrams are labeled according to RSV F concentration as indicated). Fitting the resulting curves to a 1:1 binding stoichiometry resulted in K_a and K_d and fit values as indicated in the table below. The resulting K_D for the complex between the postfusion RSV F trimer and Palivizumab is 0.42 nM.

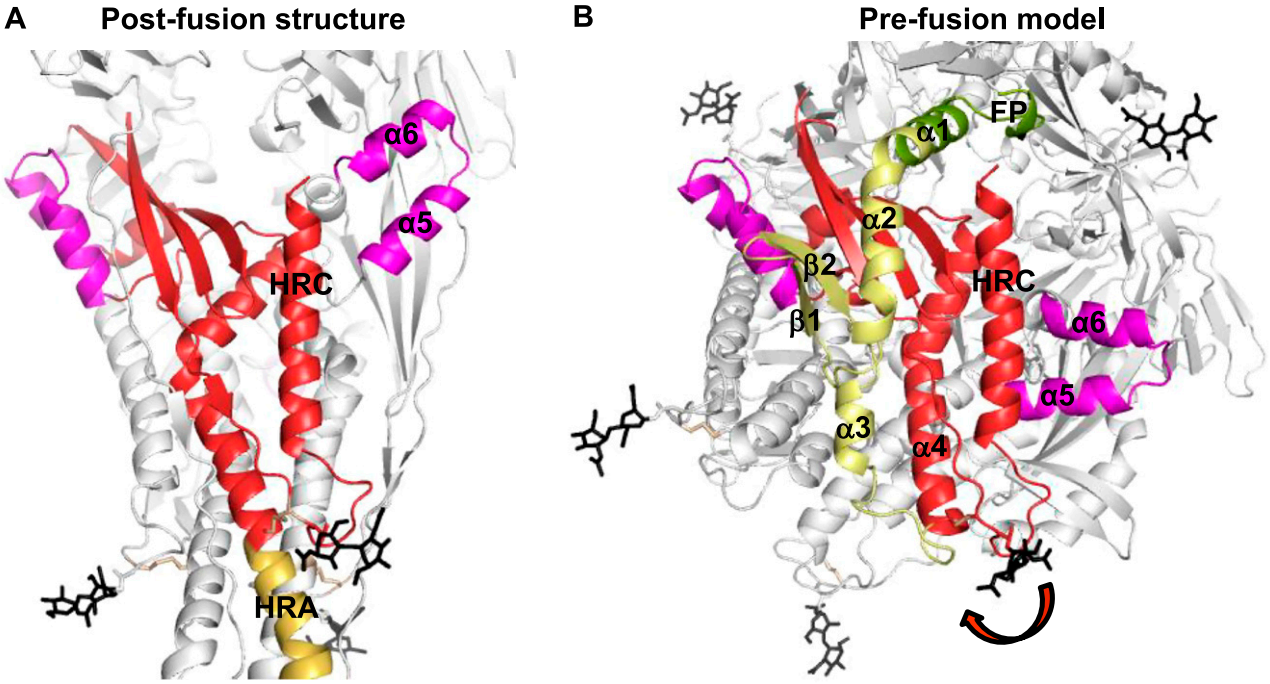

Fig. S6. Exposure of the Motavizumab epitope in the postfusion RSV F structure and prefusion RSV F model. (*A*) Domain III of the postfusion structure is highlighted in the context of the RSV F trimer. Only one domain III of the F trimer is colored; the remaining parts of RSV F are in white. Structural elements that change little between pre- and postfusion F are red; HRA, which refolds in the transition from the pre- to postfusion conformation, is yellow; and the Motavizumab epitope of each monomer is magenta. The α5 and α6 helices are labeled. (*B*) Domain III of the prefusion model colored as in *A*. The fusion peptide is green and labeled FP. In both the prefusion and postfusion structures, α5 and α6 helices are surface exposed. However, in the prefusion model, the HRC loop needs to shift to accommodate antibody binding (as indicated by the arrow).

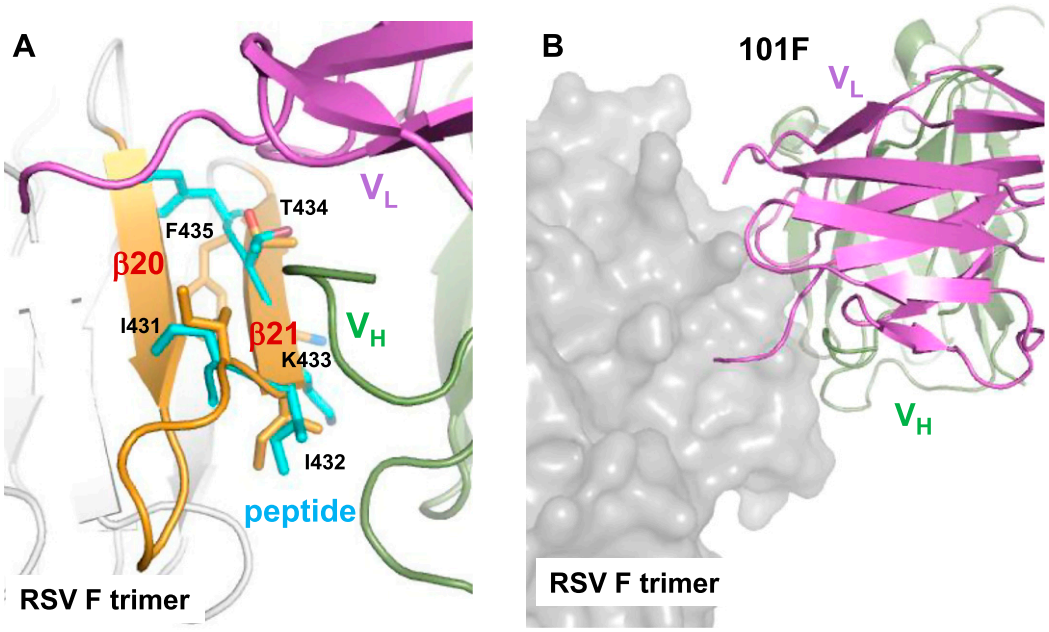

Fig. S7. Model of neutralizing antibody 101F bound to the postfusion RSV F trimer. (*A*) The peptide (cyan coil, residues 430–436) from the 101F Fab–peptide complex structure (PDB code 3O41) (1) is superposed on equivalent residues of the RSV F structure (β strands 20 and 21 in orange). Principle contact residue side chains I431, I432, K433, and T434 are exposed in the F structure and available for Fab binding. By contrast, F435, which makes contacts with the Fab in the peptide structure, is buried in the protein structure. (*B*) Ribbon representation of a model of the 101F Fab bound to the RSV F postfusion trimer. 101F Fab V_H and V_L domains are green and purple, respectively; RSV F is shown as a spacefill model in gray. The model is shown in a slightly different orientation than *A* to highlight the lack of significant clashes in the Fab-bound model.

1. McLellan JS, et al. (2010) Structure of a major antigenic site on the respiratory syncytial virus fusion glycoprotein in complex with neutralizing antibody 101F. *J Virol* 84:12236–12244.

Table S1. Crystallographic data

Data collection statistics	
Space group	P 2_1 2_1 2_1
Cell dimensions (Å)	*a* = 87.930
	b = 113.160
	c = 311.370
	α = β = γ = 90.00°
Resolution limit (Å)	50–3.2
Unique reflections	51,911
Unique reflections*	40,398
Redundancy	3.9 (3.7)‡
Overall completeness (%)	99.4 (99.4)
Overall completeness (%)*	77.0 (26.7)
<I/σ>	12.2 (2.2)
R_{sym} (%)	7.7 (71.0)
Refinement statistics†	
Polypeptide chains	3
Protein atoms	10,398
Residues in allowed regions of the Ramachandran plot (%)	98.5
Residues in most favored regions of Ramachandran plot (%)	83.5
RMSD bond lengths (Å)	0.021
RMSD bond angles (deg)	2.053
Mean B values (Å^2)	15.71
Resolution range (Å)	30–3.2
R_{work} (%)	23.1 (34.9)
R_{free} (%)	26.6 (40.2)

*Statistics for the data after anisotropic correction.
†Refinement values for the data after anisotropic correction.
‡Values in parentheses refer to data in the highest resolution shell.

Table S2. Neutralizing epitopes of RSV F*

Site[†]	mAb	Residues	Method	Reference
A	11	N268I	Escape[‡]	(1)
A	151	K272N	Escape	(2)
A	1129	S275F	Escape	(2)
A	1153	N262S	Escape	(2)
A	1200	K272N	Escape	(2)
A	1214	N276Y	Escape	(2)
A	1237	N276Y	Escape	(2)
A	47F	N262Y, N268I	Escape	(3)
A	7C2	K272E, K272T	Escape	(1)
A	B4	K272T	Escape	(1)
A	Fab 19[§]	I266M	Escape	(2)
A	AK13A2	N262Y	Escape	(1)
A	PVZ[¶]	K272M, K272Q, N268I	Escape	(4)
A	PVZ[¶]	K272M, K272T, S275F	Engineered[‖]	(5)
A	MVZ**	N262, N268, D269, K272, S275	Structure[††]	(6)
C	7.936	I432T, K433T, V447A	Escape	(7)
C	9.432	S436F	Escape	(7)
C	19[§]	R429S	Escape	(1)
C	19[§]	R429K, R429S, G430A	Engineered	(5)
C	20	R429S	Escape	(1)
C	101F	K433T	Escape	(8)
C	101F	K433D, K433L, K433N, K433Q, K433R	Engineered	(5)
C	101F	R429, I431, I432, K433, T434, F435, S436, N437	Structure	(9)

*Results of studies using peptide binding or peptide inhibition are not included in this table.
[†]Sites are based on the competition and cross-neutralization analysis of Beeler et al. (10).
[‡]An escape mutation is included if it is the sole mutation in an antibody-resistant strain.
[§]Fab19 and 19 are unrelated antibodies. The similar names are coincidental.
[¶]Palivizumab.
[‖]Engineered mutations in intact recombinant RSV F that allowed intact processing, full fusion activity, and reduced monoclonal antibody binding to less than 15% of wild type are included.
**Motavizumab.
[††]Residues from peptides in peptide–Fab complex structures are included if either their side chain or backbone atoms make significant contact with the antibody. The biological significance of the peptide–antibody interactions observed in these structural studies has been confirmed by other techniques.

1. Arbiza J, et al. (1992) Characterization of two antigenic sites recognized by neutralizing monoclonal antibodies directed against the fusion glycoprotein of human respiratory syncytial virus. *J Gen Virol* 73:2225–2234.
2. Crowe JE, et al. (1998) Monoclonal antibody-resistant mutants selected with a respiratory syncytial virus-neutralizing human antibody fab fragment (Fab 19) define a unique epitope on the fusion (F) glycoprotein. *Virology* 252:373–375.
3. López JA, Peñas C, García-Barreno B, Melero JA, Portela A (1990) Location of a highly conserved neutralizing epitope in the F glycoprotein of human respiratory syncytial virus. *J Virol* 64:927–930.
4. Zhao X, Chen FP, Sullender WM (2004) Respiratory syncytial virus escape mutant derived in vitro resists palivizumab prophylaxis in cotton rats. *Virology* 318:608–612.
5. Liu C, et al. (2007) Relationship between the loss of neutralizing antibody binding and fusion activity of the F protein of human respiratory syncytial virus. *Virol J* 4:71.
6. McLellan JS, et al. (2010) Structural basis of respiratory syncytial virus neutralization by motavizumab. *Nat Struct Mol Biol* 17:248–250.
7. López JA, et al. (1998) Antigenic structure of human respiratory syncytial virus fusion glycoprotein. *J Virol* 72:6922–6928.
8. Wu SJ, et al. (2007) Characterization of the epitope for anti-human respiratory syncytial virus F protein monoclonal antibody 101F using synthetic peptides and genetic approaches. *J Gen Virol* 88:2719–2723.
9. McLellan JS, et al. (2010) Structure of a major antigenic site on the respiratory syncytial virus fusion glycoprotein in complex with neutralizing antibody 101F. *J Virol* 84:12236–12244.
10. Beeler JA, van Wyke Coelingh K (1989) Neutralization epitopes of the F glycoprotein of respiratory syncytial virus: Effect of mutation upon fusion function. *J Virol* 63:2941–2950.